Emergent Mating Topologies in Spatially Structured Genetic Algorithms

Joshua L. Payne
Dept. of Computer Science
University of Vermont
Burlington, VT 05405
802-656-9116
jpayne@cems.uvm.edu

Margaret J. Eppstein
Dept. of Computer Science
University of Vermont
Burlington, VT 05405
802-656-1918
Maggie.Eppstein@uvm.edu

ABSTRACT
The application of network analysis to emergent mating topologies in spatially structured genetic algorithms is presented in this preliminary study as a framework for inferring evolutionary dynamics in recombinant evolutionary search. Emergent mating topologies of populations evolving on regular, scale-free, and small-world imposed spatial topologies are analyzed. When the population evolves on a scale-free imposed spatial topology, the topology of mating interactions is also found to be scale-free. However, due to the random initial placement of individuals in the spatial topology, the scale-free mating topology lacks correlation between fitness and vertex connectivity, resulting in highly variable convergence rates. Scale-free mating topologies are also shown to emerge on regular imposed spatial topologies under high selection pressure. Since these scale-free emergent mating topologies self-organize such that the most-fit individuals are inherently located in highly connected vertices, such emergent mating topologies are shown to promote rapid convergence on the test problem considered herein. The emergent mating topologies of populations evolving on small-world imposed spatial topologies are not found to possess scale-free or small-world characteristics. However, due to the decrease in the characteristic path length of the emergent mating topology, the rate of population convergence is shown to increase as the imposed spatial topology is tuned from regular to small-world.

Categories and Subject Descriptors
I.2.8 Artificial Intelligence [**Problem Solving, Control Methods, and Search**]: *Heuristic Methods*

General Terms
Algorithms, Performance, Design, Experimentation

Keywords
Emergence, Genetic Algorithms, Mating Topologies, Network Analysis, Scale-Free, Self-Organization, Small-World

GECCO'06, July 8–12, 2006, Seattle, Washington, USA.

1. INTRODUCTION
There has been a recent surge of interest in modeling and analyzing interactions in complex systems as networks. Such analysis has provided an understanding of the mechanisms by which complex systems are generated and has offered useful insight into their dynamics and underlying topological structure. Many seemingly disparate systems, both natural and manmade, have been shown to possess "small-world" and/or "scale-free" topological characteristics.

The realization that the topologies of many real-world systems possess similar attributes began with the seminal work of Watts and Strogatz [22]. Prior to this work, the connection topologies of real-world systems were typically modeled as either regular graphs or completely random graphs. However, Watts and Strogatz found that the interaction topologies of several biological, technological, and societal systems could not be captured by either of these models; these systems had characteristics that left them somewhere in the middle of the two extremes. In particular, these topologies were found to have a high degree of clustering among vertices, reminiscent of a regular graph, but a short characteristic path length between vertices, reminiscent of a random graph. In order to model such systems, Watts and Strogatz introduced a simple algorithm that produced networks with these topological characteristics and named them "small-world." The neural network of the worm *Caenorhabditis elegans*, the collaboration topology of film actors, the power grid of the Western United States [22], email networks [6], and the cerebral cortex of primates [21] are just a few examples of systems that have been shown to possess small-world characteristics.

Shortly after the introduction of small-world networks, Albert and Barabási investigated the connection topology of the World Wide Web (WWW) and found that the distribution of vertex connectivity did not follow the Poisson distribution predicted by the random and small-world models [2]. The connection topology of the WWW obeyed a power law, where the probability a given vertex had k connections was governed by the relationship $P(k) \sim k^{-\gamma}$. This was an important finding as it showed that while the majority of vertices had very few links, a few vertices possessed the majority of links, acting as hubs in the network. These networks were termed "scale-free" and it was subsequently shown that this connection topology is quite ubiquitous in natural and manmade systems. The internet [20], human sexual interactions

[14], metabolic networks [10], protein-protein interactions [11], and semantic relationships between words in the English language [17] have all been shown to possess a scale-free distribution of vertex connectivity.

Understanding the structural characteristics of interaction networks in complex systems has provided useful insight into their dynamics. The discovery of the scale-free distribution of vertex connectivity in the map of the internet provided an understanding of both the robustness of this system to random failure and its vulnerability to targeted attacks [3]. The finding that the distribution of human sexual interactions in Sweden obeyed a power-law provided insight into how to possibly design more effective methods for public health intervention and educational campaigns [14]. The shortcuts found in small-world networks, such as societal interactions, provided insight into how information spreads within a population [12], knowledge that has proved very useful to both epidemiologists and marketing strategists in understanding the spread of disease and consumer awareness of new products

Analysis of the structural properties of spatial interaction networks in evolving artificial populations has received attention in the evolutionary computation and artificial life communities as well. There has been a growing appreciation for the influence of population structure on evolutionary dynamics in recent years; metapopulation (*i.e.* island model) [5] and cellular [1],[9],[15],[18],[23] spatial structures have been thoroughly studied and have proven useful in maintaining population diversity and curbing premature convergence. More recently, the effect of small-world and scale-free population structures on the dynamics of evolutionary algorithms has been examined, focusing primarily on the structural characteristics of the network of *potential* mating interactions (*i.e.* population structure). In particular, the evolutionary dynamics of populations evolving on scale-free imposed spatial topologies have been explored in the context of evolutionary game theory [13], and the evolutionary dynamics of populations evolving on both small-world and scale-free imposed spatial topologies have been investigated with genetic algorithms (GA) [8]. However, network analysis has yet to be applied to the topology of *actual* mating interactions that *emerge* when a population evolves on a given imposed spatial topology. Distinguishing between the *imposed spatial topology* (IST) upon which the population evolves and the *emergent mating topology* (EMT) is important since it is ultimately the EMT that governs the dynamics of a population-based optimization algorithm in recombinant evolutionary search. Understanding the structure of the EMT may provide more direct insight regarding the adaptability of a population and the rate at which genetic information disseminates throughout a population. Thus, the EMT may prove to be the more relevant topology to investigate.

In the following, the EMT of a generational GA is investigated on a variety of ISTs: regular graphs with various mating neighborhood sizes (from nearest neighbor to panmictic), small-world graphs, and scale-free graphs. The primary goal of this preliminary study is to assess the structural characteristics of these emergent mating networks. None of the EMTs found were small-world, but EMTs from both scale-free and regular ISTs with sufficient selection pressure were found to be scale-free, although with different relationships between fitness and vertex connectivity. A few preliminary results regarding some implications on evolutionary dynamics are discussed, although the relationship between the structural characteristics of the emergent mating networks and their function will be addressed more fully in future research.

2. METHODS

2.1 Network Analysis of EMTs

EMTs were modeled as a labeled graph, **G**, with individuals represented as vertices $v_1, v_2, \ldots, v_\mu$ where μ is the population size. Mating interactions between individuals were represented as edges between vertices, captured in a symmetric adjacency matrix, **A**, such that $a_{i,j} = 1$ if individuals i and j mate with one another in a given generation and $a_{i,j} = 0$ otherwise. Edge multiplicity was ignored in this study, though this information could easily be incorporated by weighting each edge by the number of mating interactions that took place between two individuals.

Three metrics were computed to assess the structural properties of the EMT: the probability distribution of vertex connectivity, $P(k)$, the clustering coefficient C, and the characteristic path length L. $P(k)$ is a probability distribution function that depicts the frequency with which a given vertex has k connections. For a given vertex i connected to k_i nodes, the clustering coefficient of vertex i, C_i, is the ratio between the number of edges, E_i, that actually exist between the k_i nodes and the number of edges that could potentially exist between the k_i nodes. Thus,

$$C_i = \frac{2E_i}{k_i\left(k_i - 1\right)} \tag{1}$$

and the clustering coefficient for the entire EMT is given by,

$$C = \frac{\sum_{\forall i \in EMT} C_i}{N} \tag{2}$$

where N is the total number of vertices in the EMT. L is defined as the number of edges in the shortest path between two vertices, averaged over all pairs of vertices.

An EMT was considered scale-free if a strong linear correlation between the logarithm of the probability of vertex connectivity ($P(k)$) and the logarithm of vertex connectivity (k) was found. The linearity of the correlation was determined by visual inspection on a log-log plot and quantified by the proportion of explained variation (R^2) between $\log(P(k))$ and $\log(k)$. Based on preliminary experimentation, an $R^2 > 0.96$ was used as a threshold to delineate between scale-free distributions of vertex connectivity and non-scale-free distributions of vertex connectivity (for lower R^2, the log-log plots visually appeared decidedly non-linear, as in Fig. 1, open circles). An EMT was considered small-world if $C >> C_{rand}$ and $L \approx L_{rand}$, where C_{rand} and L_{rand} are the clustering coefficient and characteristic path length, respectively, of a random graph with the same number of vertices (N) and mean vertex connectivity ($\langle k \rangle$) [22]. Metrics for random graphs were approximated analytically [22] as

$$C_{rand} \approx \frac{\langle k \rangle}{N} \tag{3}$$

and

$$L_{rand} \approx \frac{\ln(N)}{\ln(\langle k \rangle)} \quad (4)$$

2.2 Experimental Design

A generational GA was used to optimize a single 100-variable binary knapsack problem in all experiments, wherein fitness was minimized. While preliminary experimentation using other binary knapsack problems and alternative benchmark fitness functions produced qualitatively similar results, attention is restricted herein to a single problem for the sake of clarity. The GA used single-point crossover (p_{cross} = 0.85) and bitwise mutation (p_{mut} = 0.05). The single best individual was allowed to survive each generation without undergoing any genetic operations. Selection probabilities were assigned using a nonlinear rank-based function. The probability an individual of rank i was selected as a parent was calculated as

$$p_{sel}(i) = \frac{i^{\alpha}}{\sum_{\forall i \in N} i^{\alpha}} \quad (5)$$

where N consists of all the individuals in the mating neighborhood of individual i and $0 \leq \alpha \leq 1$. Thus, parent selection was based solely on relative fitness; no assortative mating preferences were employed. Rank was ordered such that the most-fit individual had the lowest rank and the least-fit individual had the highest. A tie in rank resulted in equal probability of selection. Stochastic universal sampling [7] was employed as the selection mechanism. All experiments were performed in Matlab v.7.0 [16].

EMTs were analyzed on the following ISTs: regular graphs, scale-free graphs, and small-world graphs. These ISTs are defined as follows. The regular graph ISTs were represented as square lattices with periodic boundary conditions, with additional edges added between all vertices within rectangular neighborhoods of a specified mating radius (r) centered on each vertex i (including edges from a vertex to itself). Nearest neighbor interactions in a cellular genetic algorithm thus correspond to r = 1, k = 9, while panmictic GAs correspond to $r = \mu/2 - 1$, $k = \mu$ (i.e., complete graphs). Increasing the size of the mating radius has the effect of increasing selection pressure.

Scale-free ISTs were generated according to the preferential attachment model of Albert and Barabási [4]. The topology was created incrementally such that new vertices were sequentially added to the IST with a bias toward already highly connected vertices. Formally, the topology was generated by adding new nodes to the IST one at a time until a maximum number of vertices was reached. Here, the maximum number of vertices was simply the population size (μ) since only one vertex was needed per individual. When a new node was introduced to the IST, it attached to a node i having vertex connectivity k_i with probability $\prod(k_i)$ according to:

$$\prod(k_i) = \frac{k_i}{\sum_{\forall j \in IST} k_j} \quad (6)$$

Small-world ISTs were generated according to the rewiring algorithm of Watts and Strogatz [22], as follows. The IST was initialized as a ring of μ vertices where each vertex was connected to its k = 10 nearest neighbors. Each vertex was then visited one at a time in a clockwise fashion and the edge that connected that vertex to its nearest neighbor was rewired to a randomly chosen node in the topology with probability p. Duplicate edges were forbidden. The algorithm then considered edges joining more distant neighbors in the same clockwise manner. This process repeated itself until every edge had been considered for rewiring exactly once. Since edges are rewired at random, and from any given vertex there are more distant vertices than local vertices, such rewiring forms "shortcuts" in the topology. EMTs were analyzed from ISTs across the entire range of $p \in [0,1]$, although only those in the middle of this range (e.g., $p \in$ [5e-3,1e-1]) have small-world characteristics.

For experiments on all types of ISTs, the initial population was distributed randomly on the IST without regard to fitness (as in [8]) for the same ten random initial populations for each given population size and experiment (*i.e.*, wherever possible, paired replications were performed in which experiments were initialized with identical initial populations). On each of these ISTs, ten replications were performed for each initial population, for a total of 100 trials per IST per experiment. Further details of the various experiments are provided in the next section.

3. EXPERIMENTAL RESULTS

3.1 EMTs from Regular ISTs

EMTs were analyzed on regular ISTs with mating neighborhood sizes varied from nearest neighbor interactions to panmictic. EMTs were examined for both scale-free and small-world characteristics, as follows.

For examining whether or not the EMTs were scale-free, we used a large population size of 102,400 individuals (320×320) in order to encourage the distribution, $P(k)$, to span a greater range of k, since $P(k) \geq 1/\mu$. (However, smaller populations exhibited qualitatively similar topologies). Three values of α ($\alpha \in \{1/5,1/3,1/2\}$) and 8 mating radii ($r \in \{1,2,3,4,5,10,50,$ panmictic$\}$ were investigated. Increasing either α or the mating radius increases selection pressure.

Selection pressure was found to affect the emergence of scale-free mating topologies when the population evolved on a regular IST. When α = 1/2, the EMTs from nearest neighbor interactions (r *=1,* k = 9) were not scale-free, while the EMTs from panmictic interactions ($r = \mu/2$-1, $k = \mu$) were consistently scale-free (Figure 1, Table 1). For mating neighborhoods larger than strict nearest neighbor interactions ($r \geq 2$, $k \geq 25$), a scale-free topology consistently emerged for α = 1/2 and α = 1/3 (Figure 2a). However, for α = 1/5, selection pressure was too low to promote the emergence of a scale-free EMT for any mating radius (Figure 2a). For all three values of α considered, the proportion of explained variation (R^2) between the logarithm of $P(k)$ and the logarithm of k briefly peaked for $2 \geq r \geq 5$ (Figure 2a), but the importance of this trend is uncertain. Increasing either α or r decreased the parameter (γ) governing the scale-free vertex

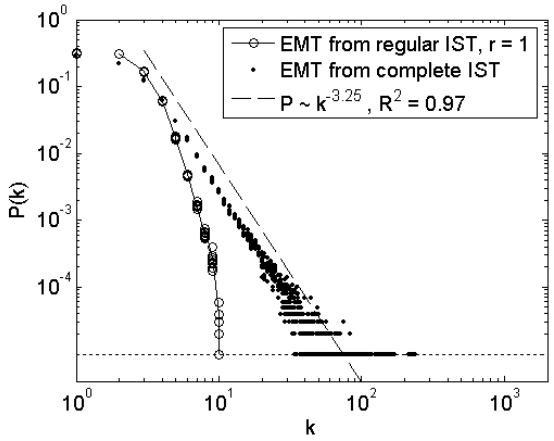

Figure. 1. Distribution of vertex connectivity, P(*k*), of EMTs from regular ISTs with nearest neighbor interactions (*r* = 1, open circles) and panmictic interactions on a complete graph (*r* = μ/2-1, black dots). Data summarizes 10 replications for each of 10 different initial populations with α = 1/2, μ = 102,400. The best-fit line of the scale-free EMT is offset to the right for visual clarity. The horizontal dotted line represents the minimum possible *P*(*k*), which is equivalent to 1/μ. Note the log-log scale.

connectivity distribution $\left(P(k) \sim k^{-\gamma}\right)$ (Figure 2b). That is, higher selection pressure caused higher connectivity in the hubs of the emergent scale-free mating topologies.

In additional experiments (not shown), we found that as the absolute mating neighborhood size increased, the selection pressure increased, and the parameter governing the emergent power-law distribution of connectivity, γ, decreased, regardless of the overall domain size. Thus, it appears that the *absolute* mating neighborhood size, rather than the *relative* neighborhood to domain size, governs the distribution of connectivity, *P*(*k*), in the scale-free EMT, since the absolute size of the mating radius determines how many potential mating interactions a given individual has.

For examining whether the EMTs possessed small-world characteristics, experiments were limited to population sizes of 2500, α = 1/2, and $r \in \{1,2,\text{panmictic}\}$, for computational reasons. As the size of the mating neighborhood increased, both the characteristic path length (*L*) and the clustering coefficient (*C*) decreased (Table 2). With small mating neighborhoods ($r \leq 2$), $L \approx 2.4 \cdot L_{rand}$, so these cannot be considered small-world, while at the other extreme (panmixia) $C \approx 1.25 \cdot C_{rand}$, so these are also not small-world (Table 2). It is possible that for some intermediate neighborhood size the EMT would be small-world, but this has not yet been demonstrated.

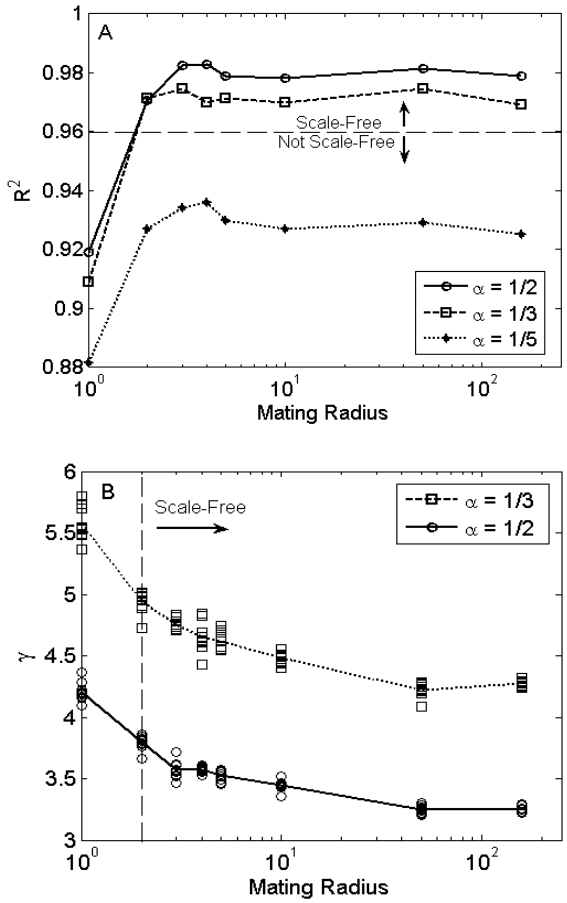

Figure 2. (A) Effect of increasing the mating radius (*r*) on the proportion of explained variation, R^2, between the log(*P*(*k*)) and the log(*k*) for α = 1/2, α = 1/3, and α = 1/5, with μ=102,400. The dashed horizontal line represents the threshold used to delineate between scale-free and non-scale-free distributions of vertex connectivity. (B) Effect of increasing the mating radius on the power law parameter, γ, governing the scale-free distribution of connectivity in the EMT. Data shown pertains to the EMT at the end of the first generation (*t* = 1). Note the log-scale on the x-axis.

3.2 EMTs from Scale-Free ISTs

Scale-free ISTs were generated as described in section 2.2. In order to increase the speed of program execution, a sparse representation of the adjacency matrix of the scale-free IST was kept in memory at all times. Due to these memory constraints, the population size was limited to 10,000 individuals. In the generated scale-free ISTs, the parameter in the power law distribution of vertex connectivity was γ = 2.68 (R^2>0.98).

Table 1. Topological characteristics of emergent mating topologies (EMT) from various imposed spatial topologies (IST), with regard to whether or not the distribution of node connectivity $P(k) = k^{-\gamma}$ in the EMT is scale-free. An EMT is considered scale-free if the proportion of explained variation (R^2) between log($P(k)$) and log(k) is greater than 0.96. For the scale-free EMTs, estimates of γ are shown as mean ± standard deviation over 100 trials.

		EMT			
		μ	**Scale-free?**	**γ**	**R^2**
IST	**Regular (r = 1)**	102,400	*No*	--	0.92
	Regular (r = 2)	102,400	*Yes*	3.79 ± 0.05	0.97
	Complete	102,400	*Yes*	3.24 ± 0.02	0.97
	Scale-Free (γ=2.68)	10,000	*Yes*	3.25 ± 0.14	0.97
	Small-World	10,000	*No*	--	0.58

Table 2. Topological characteristics of emergent mating topologies (EMT) from various imposed spatial topologies (IST), with regard to whether or not the EMT possesses small-world characteristics. An EMT is considered small-world if $L \approx L_{rand}$ and $C >> C_{rand}$. Estimates of connectivity (C) and characteristic path length (L) are shown as mean ± standard deviation over 100 trials with μ=2,500.

		EMT				
		Small-world?	***C***	***C_{rand}***	***L***	***L_{rand}***
IST	**Regular (r = 1)**	*No,* $L > L_{rand}$	0.0084 ±2.5e-3	0.0012 ±2.6e-5	22.4144 ±1.14	9.3749 ±0.09
	Regular (r = 2)	*No,* $L > L_{rand}$	0.0083 ±2.7e-3	0.0012 ±3.4e-5	22.2672 ±1.77	9.3613 ±0.16
	Complete	*No,* $C \approx C_{rand}$	0.0015 ±8e-4	0.0012 ±3e-5	8.262 ±0.22	9.218 ±0.10
	Scale-Free	*No,* $C < C_{rand}$	0.0089 ±1.3e-2	0.0210 ±6.3e-3	3.6444 ±0.67	6.6841 ±0.45
	Small-World	*No, $L > L_{rand}$*	0.0337 ±3.2e-3	0.0040 ±1.5e-6	18.7240 ±7.0e-1	3.3977 ±3.5e-4

As expected, EMTs from scale-free ISTs were also scale-free, although the slope of the average power law was steeper (γ=3.25, R^2>0.97, Table 1) than in the IST. However, the relationship between the fitness of an individual in a given node and the connectivity of that node was markedly different between the EMTs found on scale-free ISTs and complete ISTs. In order to make a fair comparison of the evolutionary dynamics between these two, we ran an additional set of paired experiments using 10 replications on each of the same 10 random initial populations, for μ = 10,000, α = 1/2. Figure 3 depicts the mean fitness of each individual with connectivity k, over all 100 trials evolving on complete ISTs and scale-free ISTs, at generations 1 and 1000. In the first generation (t = 1), there is already a strong positive correlation between good fitness and high vertex connectivity in the scale-free mating topologies that emerge from complete ISTs (Fig. 3, open circles), but not for the scale-free EMTs from scale-free ISTs (Fig. 3, × symbols). This occurs because the scale-free EMTs from complete ISTs are self-organized, such that the more connected individuals inherently possess higher fitness, whereas in the scale-free ISTs, the mating neighborhood of a given individual was determined by its random initial placement. Regardless of their fitness, the highly connected individuals in the scale-free ISTs had more mating opportunities than the less connected individuals. This difference in correlation between fitness and vertex connectivity affected evolutionary dynamics, as discussed below.

At t = 1000, the EMTs from scale-free ISTs have increased their correlation between fitness and vertex connectivity (Fig. 3, + symbols), as more-fit individuals have now had enough time to infiltrate the hubs of the IST, and thus become hubs in the EMT. Note that the maximum connectivity k also increases over time (see how the + symbols go farther to the right than the × symbols in Fig. 3), because fitter individuals in the hubs are better able to exploit the high connectivity of those hubs in the scale-free IST than their less-fit counterparts at t = 1.

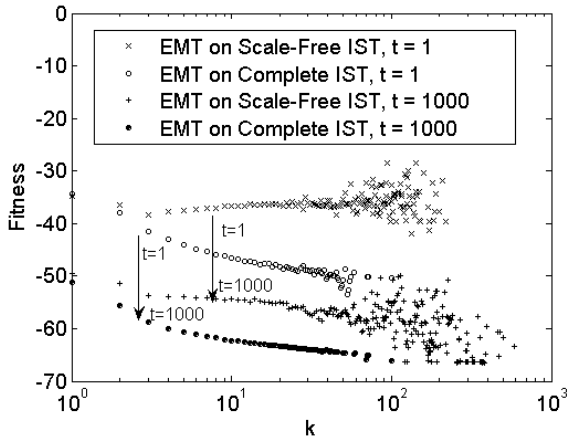

Figure 3. Relationship between vertex connectivity, *k*, and fitness in EMTs from scale-free ISTs and complete ISTs at the end of generation one (*t* = 1) and one thousand (*t* = 1000). Data summarizes ten replications for each of ten different initial populations with μ = 10,000. Fitness is being minimized. Note the log-scale on the x-axis.

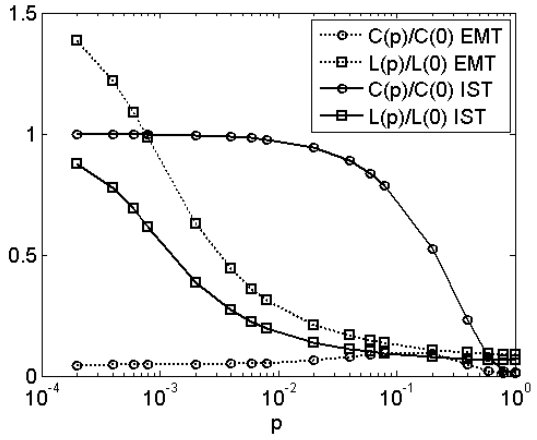

Figure 4. Comparison between the topological characteristics of small-world ISTs and the EMTs of populations evolving on these small-world ISTs for α = 1/2. Each data point represents the mean of ten replications for each of ten different initial populations. The characteristic path length (*L*) and the clustering coefficient (*C*) are normalized by the *L* and *C* of a regular graph (*p* = 0). The characteristic path length of the EMT is consistently higher than the characteristic path length of the IST upon which the population evolved, though they both follow the same trend. The clustering coefficient of the EMT remains low for all *p*, even when the clustering coefficient of the IST is high. Data shown pertains to the EMT at the end of the first generation (*t* = 1). Note the log-scale on the x-axis.

In contrast, scale-free EMTs from complete ISTs maintain a high correlation between good fitness and high vertex connectivity throughout the evolution of the population (compare Fig. 3 open and closed circles). This high correlation reduced convergence times on the complete ISTs relative to the scale-free ISTs. Surprisingly, in all 100 trials, populations on both complete and scale-free ISTs found final solutions with identical fitness (Fig. 3), so at least in this test case the more rapid convergence on the complete IST was not detrimental relative to the scale-free IST. However, it is not yet known if this result is general.

EMTs from scale-free ISTs were also examined for small-world characteristics. As with the regular ISTs, these experiments were performed on population sizes of 2,500 with α = 1/2. Although the average characteristic path lengths were actually *shorter* than those from random graphs ($L \approx 0.5 \cdot L_{rand}$, Table 2), the clustering coefficients were also lower than in random graphs ($C \approx 0.04 \cdot C_{rand}$, Table 2), so they cannot be considered small-world.

3.3 EMTs from Small-World ISTs

To investigate the EMT of a population evolving on a small-world IST, small-world ISTs with 10,000 vertices were generated as described in section 2.2 with each node initially connected to its k = 10 nearest neighbors. Once again, this population size was chosen due to the constraints incurred by keeping the adjacency matrix of the IST in memory at all times. In order to make a fair comparison between the EMT and the IST upon which the population evolved, ten parental pairings were made in each mating neighborhood in an attempt to keep the mean vertex connectivity consistent between the two topologies.

No scale-free EMT was ever found when the population evolved on a small-world IST for any *p*. However, only small-world ISTs with k = 10 were considered in this experiment. Increasing the initial vertex connectivity of the IST would increase selection pressure and may promote the emergence of scale-free EMTs as was found on regular ISTs with high vertex connectivity in section 3.1.

Surprisingly, the EMTs from small-world ISTs did *not* possess small-world characteristics (Figure 4, Table 2). This occurred as not every link in the IST necessarily manifested itself in the EMT. That is, two individuals that had the *potential* to mate due to their proximity in the IST, did not *necessarily* mate and form a link in the EMT. This resulted in the EMT having fewer total connections than the IST upon which the population evolved, despite the fact that ten parental pairings were made in each mating neighborhood. Thus, the normalized characteristic path length in the EMT is always greater, and the normalized clustering coefficient in the EMT is always less than, those of the IST from which the EMT arose (Fig. 4). Note that for small-world ISTs (e.g., $p \in$ [5e-3,1e-1]), the high clustering coefficient of the IST does not result in a high clustering coefficient in the corresponding EMT, so these EMTs cannot be considered small-world. For consistent comparison to the other ISTs studied, data for C and L are also reported for μ = 2,500, α = 1/2, p = 0.008, where it can be seen that $L \approx 5.5 \cdot L_{rand}$ and $C \approx 8.4 \cdot C_{rand}$, (Table 2), indicating that the EMT from the small-world IST is not, itself, small-world.

In a separate experiment, the convergence rates of identical populations of μ = 10,000 evolving on regular ISTs with nearest neighbor interactions (r = 1, k = 9), small-world ISTs (p = 0.008), and complete ISTs ($r = \mu/2$-1, k = μ) were compared. In all trials (data not shown), the convergence rates of populations evolving on small-world ISTs were more rapid than the convergence rates of the same populations evolving on regular ISTs (r = 1, k = 9). This result is consistent with [8]. Interestingly, the convergence rates of populations evolving on small-world ISTs were also higher than the

convergence rates of the same populations evolving on complete ISTs. Further, on this test problem, the populations evolving on small-world ISTs identified final solutions with better fitness than the final solutions obtained by the same populations evolving on either the regular or complete ISTs. This implies that the populations evolving on regular and complete ISTs were converging prematurely on local optima, although it is unclear as to whether this relationship is general. The relationship between the topological characteristics of the EMT and convergence warrants further study.

4. DISCUSSION

The goal of this preliminary study was to examine the network characteristics of emergent mating topologies in spatially structured genetic algorithms, specifically to see if they were small-world and/or scale-free. We found that the topological characteristics of emergent mating topologies can be quite different from the imposed spatial topologies upon which the population evolves. When the imposed spatial topology is scale-free, the emergent mating topology is also scale-free, but good fitness is not initially positively correlated with high connectivity. More interestingly, scale-free mating topologies were shown to emerge from regular graph imposed spatial topologies, as long as selection pressure was sufficiently high, and these exhibited a strong positive correlation between good fitness and high connectivity for at least 1000 generations on the test problem. Scale-free topologies were never found to emerge when interactions were limited to nearest neighbors on a rectangular lattice, because the selection pressure was too low. Emergent mating topologies from a variety of imposed spatial topologies (including regular graphs with small mating neighborhoods, complete graphs (panmixia), scale-free graphs, and small-world graphs) were never found to exhibit small-world characteristics, although the reasons varied for the different imposed spatial topologies. Trends in the data hint that small-world characteristics may arise from intermediate neighborhood sizes on regular graphs, but this has not yet been demonstrated. These findings have implications for the study of evolutionary dynamics in both spatially structured GAs and spatially explicit artificial life simulations.

Previous investigations of evolutionary dynamics on scale-free imposed spatial topologies [8],[13] have shown that if an individual of high fitness could successfully infiltrate one of the hubs of the scale-free topology, then that individual's genetic information would disseminate rapidly throughout the population. However, when the imposed spatial topology is scale-free, there is initially no positive correlation between good fitness and high vertex connectivity. Here, we have shown that self-organizing scale-free mating topologies spontaneously emerge from *regular* imposed spatial topologies, and inherently have a strong correlation between good fitness and high vertex connectivity. Thus, in these self-organizing scale-free mating topologies, fortuitous genetic combinations are quickly communicated throughout the population. Such swift dissemination of advantageous genetic information has implications for rapid, possibly premature, convergence.

In [8], it was also shown that the rate of convergence of populations evolving on small-world imposed spatial topologies increased as the probability of rewiring (p) increased. This is due to the shortcuts that are formed in the spatial topology as edges are rewired, which decreases the characteristic path length and allows for the spread of genetic information over longer spatial scales. In the current study, we have shown that the emergent mating topologies from small-world imposed spatial topologies are not, themselves, small-world due to their high characteristic path lengths and low clustering coefficients. However, since the characteristic path lengths of the emergent mating topologies do decrease with increased probability of rewiring, increasing p nevertheless has the effect of increasing the population convergence rate.

We also found that the spatial scale of individual mating interactions directly affected the structure of the emergent mating topology. As expected, our results confirm that the localization of individual interactions (commonly employed in both cellular genetic algorithms [1],[9],[15],[18],[23] and artificial life simulations [19]) gives rise to a long characteristic path length in the emergent mating topology. As a result, genetic information remains quite localized and travels slowly across longer spatial scales, giving rise to fundamentally different evolutionary dynamics than found in randomly mixing populations. Further, the results of this study show that the connectivity distribution, $P(k)$, of scale-free emergent mating topologies from regular imposed spatial topologies is governed by absolute, as opposed to relative, mating neighborhood size. Since different absolute mating neighborhood sizes produce emergent mating topologies which yield dramatically different evolutionary dynamics, the results of this study suggest that care should be taken in choosing biologically meaningful mating neighborhoods in spatially explicit artificial life simulations.

5. SUMMARY

In recent years, there has been a growing appreciation for the important influence of spatial relationships on evolutionary dynamics. Consequently, a variety of spatially explicit imposed population structures are being explored for use in GAs [1],[8],[23]. Our results, while preliminary, indicate that analysis of the network characteristics of the *emergent* (rather than imposed) mating topologies may provide valuable insight regarding evolutionary dynamics in populations, both natural and artificial. This method can expose underlying similarities and differences in the evolutionary dynamics produced on various disparate imposed spatial topologies. While the main focus of this study was to understand the structural characteristics of the mating topologies that emerge from various imposed spatial topologies, future endeavors will more fully explore the relationship between the structure of these emergent topologies and evolutionary dynamics. Further, future work will expand upon the results presented in this preliminary study by investigating emergent mating topologies and their dynamics on a broader range of test problems, and using alternative ranking functions and selection operators. We are particularly interested in the implications for adaptability in changing environments.

6. Acknowledgments

This work was supported in part by a graduate research assistantship funded by DOE-FG02-00ER45828 awarded by the US Department of Energy through its EPSCoR Program.

7. References

[1] Alba, E. & Dorronsoro, B. The exploration/exploitation tradeoff in dynamic cellular genetic algorithms. *IEEE Transactions on Evolutionary Computation*, 9, 2, (2005), 126-142.

[2] Albert, R., Jeong, H., & Barabási, A.L. Diameter of the World-Wide Web. *Nature*, 401 (1999), 130-131.

[3] Albert, R., Jeong, H., & Barabási, A.L. Error and attack tolerance of complex networks. *Nature*, 406 (2000), 378-381.

[4] Barabási, A.L. & Albert, R. Emergence of scaling in random networks. *Science*, 286 (1999), 509-512.

[5] Cohoon, J.P., Hedge, S.U., Martin, W.N., & Richards, D.S. Punctuated Equilibria: a parallel genetic algorithm. In *Proc. 2nd International Conference on Genetic Algorithms* (Pittsburgh, PA, 1987). Erlbaum, Hillsdale, N.J., 1987, 148-154.

[6] Ebel, H., Mielsch, L., & Bornholdt, S. Scale-free topology of e-mail networks. *Physical Review E*, 66 (2002) 035103(R).

[7] Eiben, A.E. & Smith, J.E. *Introduction to Evolutionary Computing*. Springer-Verlag: Berlin (2003).

[8] Giacobini, M., Tomassini, M., & Tettamanzi, A. Takeover time curves in random and small-world structured populations. In *Proc. Genetic and Evolutionary Computation Conference* (Washington, D.C., June 25-29, 2005). ACM Press, New York, N.Y., 2005, 1333-1340.

[9] Gordon, V. & Whitely, D. Serial and parallel genetic algorithms as function optimizers. (Urbana-Champaign, IL, July, 1993). Morgan Kaufman, San Mateo, CA, 1993, 177-183.

[10] Jeong, H., Tombor, H., Albert, R., Oltavi, Z.N., & Barabási, A.L. The large-scale organization of metabolic networks. *Nature*, 407 (2000), 651-654.

[11] Jeong, H., Mason, S.P., Barabási, A.L., & Oltvai, Z.N. Lethality and centrality in protein networks. *Nature*, 411 (2001), 41-42.

[12] Kuperman, M., & Abramson, G. Small-world effect in an epidemiological model. *Physical Review Letters*, 86 (2001), 2909-2912.

[13] Lieberman, E., Hauert, C., & Nowak, M.A. Evolutionary dynamics on graphs. *Nature*, 433 (2005), 312-316.

[14] Liljeros, F., Edling, C.R., Amaral, L.A.N., Stanely, H.E., & Åberg, Y. The web of human sexual contacts. *Nature*, 411 (2001), 907-908.

[15] Manderick, B. & Spiessens, P. Fine-grained parallel genetic algorithms. In *Proc. 3rd Int. Conf. on Genetic Algorithms* (Fairfax, VA, June 1989). Morgan Kaufman, San Mateo, CA, 1989, 428-433.

[16] MathWorks. 24 Prime Park Way, Natick MA 01760-1500 (2004).

[17] Motter, A.E., de Moura, A.P.S., Lai, Y.C., & Dasgupta, P. Topology of the conceptual network of language. *Physical Review E*, 65 (2002), 065102(R).

[18] Sarma, J., & De Jong, K. An analysis of the effect of neighborhood size and shape on local selection algorithms. In *Proc. Int. Conf. Parallel Prob. Solving from Nature IV* (Berlin, German, September 22 – 26, 1996). Springer-Verlag, Berlin, Germany, 1996, 236-244.

[19] Sayama, H., Kaufman, L., & Bar-Yam, Y. Symmetry breaking and coarsening in spatially distributed evolutionary processes including sexual reproduction and disruptive selection. *Physical Review E*, 62 (2000), 7065-7069.

[20] Siganos, G, Faloutsos, M., Faloutsos, P., & Faloutsos, C. Power laws and the AS-level internet topology. *IEEE/ACM Transactions on Networking*, 11,4 (2003), 514-524.

[21] Stephan, K.E., Hilgetag, C., Burns, G.A.P.C., O'Neill, M.A., Young, M.P., & Kötter, R. Computational analysis of functional connectivity between areas of primate cerebral cortex. *Phil. Trans. R. Soc. Lond. B*, 355 (2000) 111-126.

[22] Watts, D.J., & Strogatz, S.H. Collective dynamics of 'small-world' networks. *Nature*, 393 (1998), 440-442.

[23] Whitely, D. Cellular genetic algorithms. In *Proc. 5th Int. Conf. Genetic Algorithms* (Urbana-Champaign, IL, July, 1993). Morgan Kaufman, San Mateo, CA, 1993, 658.